

Semi-volatile components of PM_{2.5} in an urban environment: Volatility profiles and associated oxidative potential

Milad Pirhadi^a, Amirhosein Mousavi^a, Sina Taghvaei^a, Martin M. Shafer^b, Constantinos Sioutas^{a,*}

^a University of Southern California, Department of Civil and Environmental Engineering, Los Angeles, CA, USA

^b University of Wisconsin-Madison, Wisconsin State Laboratory of Hygiene, Madison, WI, USA

HIGHLIGHTS

- We assessed volatility profile and oxidative potential of PM_{2.5} semi-volatile components.
- Different organic species and inorganic ions showed considerable losses upon heating.
- Almost half of PM_{2.5} oxidative potential was removed by heating the aerosol to 50 °C.
- The removal of oxidative potential further increased to 75–85% upon heating to 100 °C.
- PM_{2.5} oxidative potential was highly correlated with organic species in warm and cold seasons.

ARTICLE INFO

Keywords:

PM_{2.5} oxidative potential
Semi-volatile organic compounds (SVOCs)
Gas-particle partitioning
Thermodenuder
Volatility
DCFH assay

ABSTRACT

The volatility profiles of PM_{2.5} semi-volatile compounds and relationships to the oxidative potential of urban airborne particles were investigated in central Los Angeles, CA. Ambient and thermodenuded fine (PM_{2.5}) particles were collected during both warm and cold seasons by employing the Versatile Aerosol Concentration Enrichment System (VACES) combined with a thermodenuder. When operated at 50 °C and 100 °C, the VACES/thermodenuder system removed about 50% and 75% of the PM_{2.5} vol concentration, respectively. Most of the quantified PM_{2.5} semi-volatile species including organic carbon (OC), water soluble organic carbon (WSOC), polycyclic aromatic hydrocarbons (PAHs), organic acids, n-alkanes, and levoglucosan, as well as inorganic ions (i.e., nitrate, sulfate, and ammonium) exhibited concentration losses in the ranges of 40–66% and 67–92%, respectively, as the thermodenuder temperature increased to 50 °C and 100 °C. Species in the PM_{2.5} such as elemental carbon (EC) and inorganic elements (including trace metals) were minimally impacted by the heating process – thus can be considered refractory. On average, nearly half of the PM_{2.5} oxidative potential (as measured by the dichlorodihydrofluorescein (DCFH) alveolar macrophage in vitro assay) was associated with the semi-volatile species removed by heating the aerosols to only 50 °C, highlighting the importance of this quite volatile compartment to the ambient PM_{2.5} toxicity. The fraction of PM_{2.5} oxidative potential lost upon heating the aerosols to 100 °C further increased to around 75–85%. Furthermore, we document statistically significant correlations between the PM_{2.5} oxidative potential and different semi-volatile organic compounds originating from primary and secondary sources, including OC (R_{warm} , and R_{cold}) (0.86, and 0.74), WSOC (0.60, and 0.98), PAHs (0.88, and 0.76), organic acids (0.76, and 0.88), and n-alkanes (0.67, and 0.83) in warm and cold seasons, respectively, while a strong correlation between oxidative potential and levoglucosan, a tracer of biomass burning, was observed only during the cold season ($R_{\text{cold}} = 0.81$).

1. Introduction

Prolonged exposure to elevated levels of ambient particulate matter (PM) has been widely demonstrated to be a major cause of numerous

common illnesses, including respiratory diseases, lung cancer, cardiovascular diseases, and neurodegenerative disorders (Brook et al., 2010; Cassee et al., 2013; Cheng et al., 2016). Among the different size classes of PM, many focus on ambient PM_{2.5} (i.e., particles with aerodynamic

* Corresponding author. 3620 S. Vermont Ave., Los Angeles, CA, 90089, USA.
E-mail address: sioutas@usc.edu (C. Sioutas).

<https://doi.org/10.1016/j.atmosenv.2019.117197>

Received 2 July 2019; Received in revised form 9 October 2019; Accepted 30 November 2019

Available online 2 December 2019

1352-2310/© 2019 Elsevier Ltd. All rights reserved.

diameters $< 2.5 \mu\text{m}$) due to its diverse physico-chemical characteristics, various sources, and documented enhanced adverse health consequences (Apte et al., 2018; Davidson et al., 2007; Dockery and Stone, 2007; Pope III et al., 2015; Senlin et al., 2008).

A well-documented underlying mechanism for the toxicity of PM is excessive cellular production of reactive oxygen species (ROS), resulting in an oxidative stress response and in turn, adverse health outcomes (Delfino et al., 2013; Steenhof et al., 2011). Once the concentrations of cellular ROS exceed the levels at which normal cellular antioxidant controls can maintain homeostasis, pathways leading to adverse health impacts are triggered (Li et al., 2009). Previous studies have shown associations between specific components of ambient PM and toxicity and oxidative potential, including non-volatile compounds such as redox active metals (Ercal et al., 2001; Gasser et al., 2009), and elemental carbon (EC) (Cho et al., 2005; Samara, 2017) as well as semi-volatile species such as organic carbon (OC) (Bates et al., 2019; Biswas et al., 2009; Pirhadi et al., 2018), water soluble organic carbon (WSOC) (Bae et al., 2017; Verma et al., 2009), and polycyclic aromatic hydrocarbons (PAHs) (Delgado-Saborit et al., 2011; Knecht et al., 2013). However, despite the contemporary research, there is still considerable uncertainty associated with the relative importance of these components in different urban environments.

Many studies have highlighted the abundance of semi-volatile species in common PM emission sources, such as gasoline vehicles, diesel exhaust, and wood stoves (Lipsky and Robinson, 2006; May et al., 2013a, 2013b; Robinson et al., 2010). For example, May et al. (2013a) investigating fifty-one different light duty gasoline-powered vehicles, reported that around 80% of the primary organic aerosol (POAs) emissions are semi-volatile species, which rapidly condense following emission (Charron and Harrison, 2003; Zhang et al., 2011). These species are also important precursors for the formation of secondary organic aerosols (SOAs) through their photochemical oxidation in the atmosphere, a process that transforms these primary species chemically as well as toxicologically (Fine et al., 2008; Jimenez et al., 2009; Saffari et al., 2016, 2015; Tuet et al., 2017). Few studies have specifically addressed the semi-volatile components of $\text{PM}_{2.5}$ as drivers of their toxicological characteristics.

Several studies have addressed the toxicity of certain water-soluble (e.g., WSOC) and -insoluble (e.g., PAHs) semi-volatile species (Delgado-Saborit et al., 2011; Knecht et al., 2013; Wang et al., 2013b), while ambient PM is a complicated mixture of numerous components and it is essential to find the relative role of each of the abundant individual labile species in ambient PM. Some studies have also evaluated the toxicity of semi-volatile compounds emitted from particular sources such as diesel, and biodiesel engines, immediately after emission, either in dynamometer facilities or smog chambers (Biswas et al., 2009; Gali et al., 2017; Steiner et al., 2013). However, these studies likely do not fully capture the complex nature of the semi-volatile components of real-world ambient PM, especially those with secondary origins formed during the atmospheric aging processes. Verma et al. (2011) investigated the toxicity and volatility of quasi ultrafine particles (i.e., particles with aerodynamic diameters $< 180 \text{ nm}$) in central Los Angeles and showed that semi-volatile components of quasi ultrafine PM have a considerable effect on the associated oxidative potential of particles in this size range. However, many semi-volatile organic compounds, such as SOAs, PAHs, and n-alkanes have significant mass fractions in the accumulation mode in different urban environments (Bi et al., 2005; Fine et al., 2004; Jimenez et al., 2009; Sowlat et al., 2016; Wang et al., 2009). Consequently, to more appropriately address the human health impacts of these emissions, it is critical to chemically characterize the real world ambient $\text{PM}_{2.5}$ -bound semi-volatile compounds and evaluate their associated toxicity in a representative metropolitan area like Los Angeles, which is heavily impacted by a mixture of primary and secondary pollutants (Docherty et al., 2008; Hasheminassab et al., 2014a; Ortega et al., 2016).

The primary objective of this study was to investigate the volatility

profile and toxicological characteristics of $\text{PM}_{2.5}$ semi-volatile components in a typical urban environment in central Los Angeles, CA. A Versatile Aerosol Concentration Enrichment System (VACES) was combined with a state-of-the-art thermodenuder to investigate the gas-particle partitioning of the semi-volatile compounds on collected $\text{PM}_{2.5}$ samples at 50°C and 100°C . Our study was carried out in both warm and cold seasons with the goal of assessing potential seasonal variations that would better allow for enhanced resolution of major $\text{PM}_{2.5}$ toxicity drivers. The oxidative potential of the filter-collected $\text{PM}_{2.5}$ was quantified using the fluorogenic dichlorodihydrofluorescein (DCFH) alveolar macrophage in vitro assay. This assay utilizes the fluorescent probe DCFH-DA (2',7'-dichlorodihydrofluorescein diacetate) to quantify PM oxidative activity - reactive oxygen species generated upon interaction of redox-active particle components with rat alveolar macrophage cells. The membrane-permeable DCFH-DA probe enters the macrophage cell and is de-acetylated by cytoplasmic esterases, which then allows intracellular ROS species to convert DCFH to its fluorescent form, DCF. DCFH is a broad-spectrum ROS probe, responsive to many of the cellular ROSs including hydroxyl and superoxide radicals and indirectly peroxides. This enables the quantification of biologically mediated production of ROS in response to cellular stimulation (e.g. PM exposure). The macrophage cell line NR8383 manifests all the functional characteristics of normal primary macrophages and exhibits a strong response to external stimuli (both particulate and soluble) by phagocytosis and killing (Landreman et al., 2008). Importantly, the cells exhibit oxidative burst and secrete a wide range of oxidative stress and inflammatory cytokine markers. Several epidemiological studies have documented that this in-vitro approach exhibits a robust association with airway and systemic inflammation biomarkers (Delfino et al., 2013, 2010; Wittkopp et al., 2016).

Chemical analysis on the quartz filters was performed to characterize different components of collected samples including OC, WSOC, EC, trace elements and metals, inorganic ions, PAHs, organic acids, and n-alkanes to further investigate their volatility profiles and impacts on the $\text{PM}_{2.5}$ oxidative potential. The collection of semi-volatile species on quartz filters might be subjected to negative or positive sampling artifacts (Mader et al., 2003; Subramanian et al., 2004). Negative artifacts refer to the loss of semi-volatile species during the collection period, whereas positive artifacts pertain to the adsorption of semi-volatile compounds on the quartz filters. Negative artifacts are not expected to significantly impact our reported concentrations in this study due to the low pressure drop (i.e., $< 1 \text{ kPa}$) across our quartz filter samplers (Ziková et al., 2015) as well as the implementation of an aerosol concentrator (i.e., the VACES with particulate-phase enrichment factors up to 120) that drastically decreases the volatilization losses of PM compounds (Chang et al., 2000; S. Kim et al., 2001b; Ning et al., 2006; Zhang and McMurry, 1992). Moreover, the impact of positive artifacts decreases significantly with higher PM mass loadings on the filter, a result of prolonged sampling times and/or higher PM mass concentrations (as in our case of around $2000 \mu\text{g}/\text{m}^3$ using the VACES) leading to the saturation of the adsorption sites of the quartz filters (B. M. Kim et al., 2001; Sardar et al., 2005).

2. Methodology

2.1. Sampling campaign and location

Our field experimental campaign was conducted in two seasons, a warm (August 2018), and a colder period (late December 2018 to early January 2019). The sampling periods were selected to capture the meteorological extremes in terms of ambient temperature and relative humidity (RH) and maximize the range of concentrations of the investigated chemical species (Hasheminassab et al., 2014b; Mousavi et al., 2018; Saffari et al., 2014). In the warm phase, the ambient temperature and RH were $23.7 \pm 3.1^\circ\text{C}$ and $68.6 \pm 11.8\%$, respectively, while the corresponding values in the cold period were $13.2 \pm 2.6^\circ\text{C}$ and $78.1 \pm$

11.7%, respectively. 8 sets of ambient and thermo-denuded samples (4 sets per season and temperature setting, each representing 2–3 sampling days), were collected at the Particle Instrumentation Unit (PIU) of the University of Southern California for 7 h (10 a.m.–5 pm) each day. The PIU is in downtown Los Angeles, approximately 150 m to the northeast of the I-110 freeway. The dominant southwesterly winds during the sampling campaign facilitated the transport of freshly emitted particles from the freeway to the sampling site during both seasons. Moreover, many recent studies conducted at the PIU have demonstrated that this site is representative of an urban area exposed to a mixture of primary and secondary (e.g., SOAs) PM (Mousavi et al., 2019; Sowlat et al., 2016; Taghvaei et al., 2019).

2.2. Instrumentation

Fig. 1 shows a schematic of the instrumentation setup for our sampling campaign. The VACES was used to concentrate (by an approximate factor of 20) the ambient particles; thus, decreasing the sampling time necessary to achieve required mass loading for further chemical analysis and minimizing potential time-dependent alterations of the collected PM. More detailed information on the VACES can be found in our previous publications (Kim et al., 2001b, 2001a; Ning et al., 2006). In brief, ambient aerosols are drawn at 300 lpm through a pre-impactor (with a cut-point diameter of 2.5 μm) and are then saturated with water vapor as they pass through the headspace of a tank of ultrapure water vapor at 30 $^{\circ}\text{C}$. The flow is then split into three parallel lines, each at 100 lpm; and each line enters a cooling tube in which the air temperature is reduced to 21–22 $^{\circ}\text{C}$. The supersaturation produced by this cooling process results

in the growth of ambient particles to about 3–3.5 μm droplets. In one of the three sampling lines, a virtual impactor with a cut-point diameter of 2 μm and a minor flow rate of 5 lpm is used to enrich the concentration of the grown particles up to 20-fold. After the virtual impactor, the aerosol stream is drawn into a diffusion dryer (Model 3620, TSI Inc., USA) by the means of a vacuum pump (Model 2067; GAST Manufacturing, USA) to remove the excess moisture and decrease the RH to around 40–50%. Several earlier studies have shown that the chemical composition of ambient PM, including refractory and semi-volatile components, is preserved during the concentration enrichment process by the VACES (S. Kim et al., 2001a, 2001b; Pirhadi et al., 2019; Saarikoski et al., 2014; Zhao et al., 2005). In the “thermo-denuded line”, the two minor flows of the first-stage virtual impactors were combined to provide 15 lpm total intake flow for the second-stage mini virtual impactor operating with a minor flow of 1.5 lpm and a cut-point diameter of 2 μm . This two-stage virtual impactor system, described first by Wang et al. (2013a), was used prior to the thermodenuder in order to match the operational flow rate of the thermodenuder (i.e., 1.5 lpm) with the concentrated ambient flow of the VACES system and increase the ambient PM concentration up to 120 times. During the experiments, the particle number concentrations were frequently (every half an hour) measured in the denuded line by the means of a portable DiSCmini (Matter Aerosol AG, Wohlen, Switzerland) to assure the approximate 120-fold concentration enrichment. As shown in Fig. 1, the ambient and denuded particles were collected in parallel on 37 mm diameter quartz filters (2 μm pore, Pall Life Sciences, USA) in two of the VACES lines: In the first line, ambient particles were collected directly after passing through the diffusion dryer, while

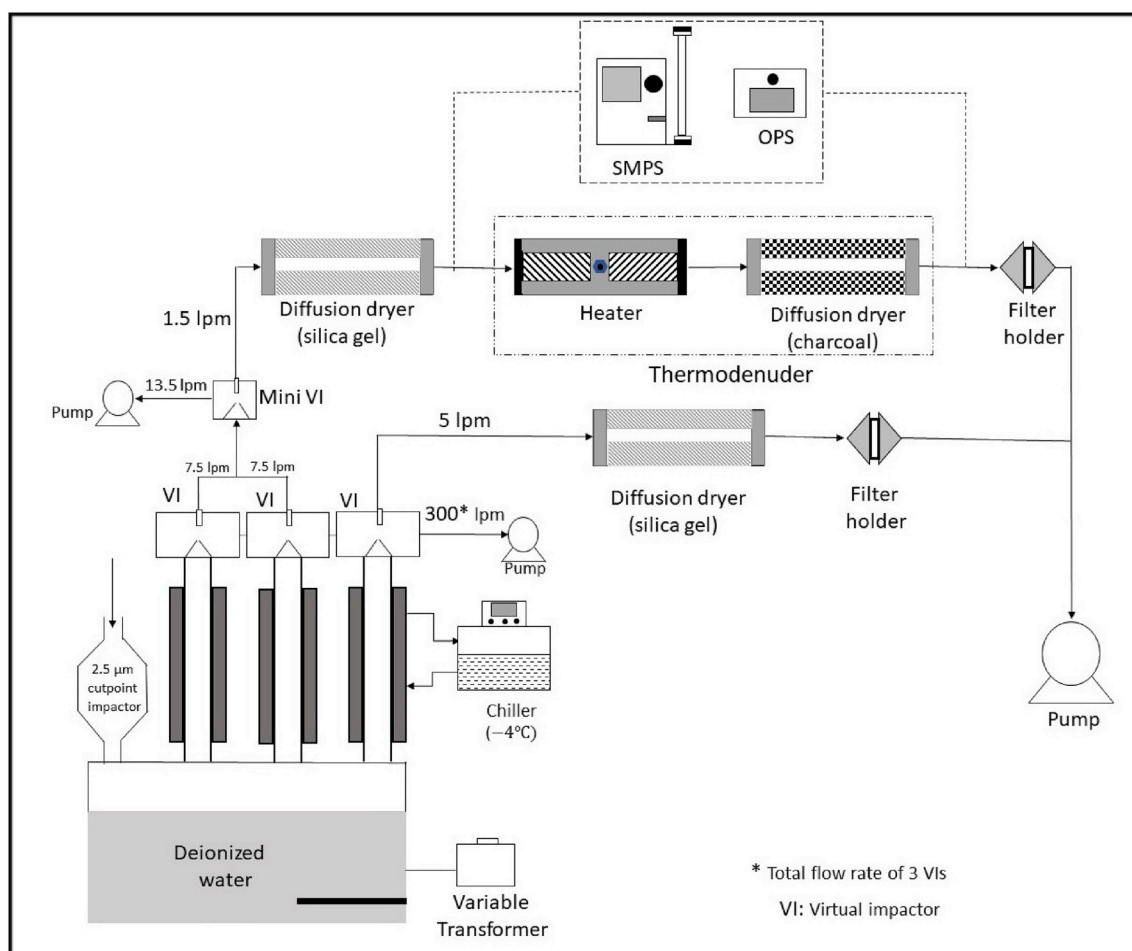


Fig. 1. Schematic of the setup for field experiments.

thermo-denuded particles were collected right after the thermodenuder (to be described in more detail in the next paragraph) at different temperature settings, in the second line of the VACES. The selection of the thermodenuder temperature settings (i.e., 50 °C and 100 °C), as will be further discussed in the results section 3.1, was based on the preliminary tests on the PM_{2.5} vol percentage losses according to the volume-based concentrations before and after the thermodenuder measured by a scanning mobility particle sizer (SMPS, Model 3936, TSI Inc., USA) connected to a condensation particle counter (CPC, 4 Model 3022A, TSI Inc., USA) for particles <0.7 µm as well as an optical particle sizer (OPS, Model 3330, TSI Inc., USA) for the size range of 0.3–2.5 µm. It was observed that heating the aerosol to roughly 50 °C resulted in approximately 50% loss of the PM_{2.5} vol, while heating the aerosol to a temperature of 100 °C resulted in around 75% loss of PM_{2.5}. Further heating to temperatures of up to 200 °C did not result in any appreciable additional loss of PM, presumably because what remains in the PM phase are mostly non-volatile refractory PM species such as EC and metals. Therefore, we selected 50 °C and 100 °C as the final temperature configurations of thermodenuder. Four sets of samples (concentrated ambient and denuded) were collected in each phase of the sampling periods (i.e., warm and cold periods), which were then analyzed for their toxicological and chemical characteristics.

We used a thermodenuder which was designed and characterized by Krasowsky et al. (2016). This thermodenuder is comprised of two main parts: the heating unit with two high-temperature heat cables (4 ft, 120 VAC, 312 Watt, McMaster-Carr, USA) that partially evaporates the semi-volatile/volatile species of the passing aerosol stream, and the adsorption unit which consists of a diffusion dryer (Model 3620, TSI Inc., USA) filled with charcoal to effectively adsorb the gas-phase components immediately after the heater and prevent their re-condensation on the surface of the denuded particles. Moreover, this thermodenuder is characterized by an aerosol residence time of 13 s, allowing a better thermal equilibration in comparison to that achieved in the previous studies such as Verma et al. (2011) with a residence time of 0.7 s, and commercially available thermodenuders developed by TSI (Model 3065) and Dekati (Model ELA 111 and 230) companies with residence times up to 1.5 s. As reported by Riipinen et al. (2010) and Saleh et al. (2011), the required thermodenuder residence time to reach the thermal equilibrium decreases significantly with increasing the aerosol concentration. Thus, for the highly concentrated aerosols collected by the 2-stage VACES (enriched in concentration up to 120 times) in our study, the 13 s of residence time would be sufficient to allow for aerosol thermal equilibration. This range of thermodenuder residence times (i.e., 10–20 s) has also been used in the earlier studies (An et al., 2007; Huffman et al., 2008; Riipinen et al., 2010; Saleh et al., 2011). Further technical details regarding the thermodenuder performance is available in Krasowsky et al. (2016).

2.3. Chemical analysis

The PM collected on the quartz filters (i.e., both denuded and ambient samples) were analyzed for their chemical constituents including inorganic ions, inorganic elements, EC, OC, WSOC, and a large suite of specific organic compounds at the Wisconsin State Laboratory of Hygiene (WSLH). The EC and OC content of the samples were determined by the means of a OC/EC field analyzer (Sunset Laboratory Inc., USA), using the Thermal Optical Transmission (TOT) method of the National Institute for Occupational Safety and Health (NIOSH) (Birch and Cary, 1996). The EC/OC determination of the PM is performed directly from a punch of the quartz filter as is standard practice in the TOT/NIOSH method. All insoluble and soluble carbonaceous species are addressed by the high-temperature combustion; thus, there is no differentiation into soluble and insoluble pools. Soluble anions (chloride, nitrate, sulfate and phosphate) and cations (ammonium, sodium, potassium) were determined using Ion Chromatography (IC, Dionex ICS 2100, and ICS 1100), from a filtered (0.45 µm) water extract (2-h with

constant agitation) of a section of the quartz filter. The soluble fraction, as is standard practice for soluble ions, is operationally defined by short water extraction and filtration. A Sievers 900 Total Organic Carbon Analyzer was employed to determine the WSOC concentrations (Stone et al., 2008), in 0.45 µm filtered water extracts of the PM from a section of the quartz filter. Specific organic species of the samples including PAHs, organic acids, n-alkanes, and levoglucosan were quantified by the Gas Chromatography/Mass Spectrometry (GC/MS) (Schauer et al., 1999). Organic speciation of the PM was performed using a mixed solvent extraction of the PM from a section of the quartz filter. This extraction is quantitative for all target organic species and can be considered a total measurement (directly comparable to the EC/OC, macrophage ROS, and inorganic speciation (ICPMS)). Finally, the total elemental content of the samples (50 elements) was quantified by magnetic-sector inductively coupled plasma mass spectrometer (MS-ICPMS) from a section of the quartz filter (Herner et al., 2006) using microwave-aided mixed-acid digestion. The PM was digested with a mixture of ultrahigh-purity nitric acid (2.0 mL 16M) and ultrahigh-purity hydrochloric acid (0.5 mL 12M). Verification of quantitative recoveries was achieved using a series of NIST CRMs (Urban Particulate Matter, San Joaquin Soil, Used Auto Catalyst and Marine Sediment). Digestion of the PM is performed directly on a section of the quartz filter, thus there is no differentiation into soluble and insoluble pools and this is a total measurement (again directly comparable to the EC/OC, macrophage ROS, and organic speciation (GC/MS)).

2.4. Quantification of the PM associated oxidative potential

The oxidative potential of the PM_{2.5} samples was quantified using the fluorogenic DCFH probe in a rat alveolar macrophage model. (Landreman et al., 2008). The influence of both water soluble and insoluble PM is quantified in the macrophage ROS assay (thus directly comparable to the detailed inorganic and organic chemical speciation measurements). The PM extracts are not filtered and the cells are directly exposed to the unfiltered extract. Briefly: a section of the quartz filter was immersed in the target volume (1.5 or 2.5 mL) of Type 1 water, sonicated for 30 min and then agitated continuously for 16 h on a table-top shaker (in the dark). At the end of the 16 h of shaking, the extract suspension was again sonicated for 30 min and then immediately sub-sampled for the macrophage ROS assay. The ROS activity of the PM extracts was measured using a previously described method employing an in-vitro rat alveolar macrophage (NR8383) model and a wide spectrum ROS probe (Landreman et al., 2008; Shafer et al., 2016). In brief, the rat alveolar macrophage NR8383 (CRL-2192™) cell line was obtained from ATCC (Manassas, VA, USA) and cultured according to the manufacturer's instructions in Hams F12 medium (Sigma Aldrich, St. Louis, MO) supplemented with 15% fetal bovine serum (FBS; Hyclone, Fisher, USA) and sodium bicarbonate (1.176 g L⁻¹). Cells were maintained at 37 °C in a humidified incubator supplied with 5% CO₂. For the oxidative activity assay, non-adherent macrophage cells were harvested, centrifuged and resuspended in Salts Glucose Media (SGM) to obtain a concentration of 1,000 cells/µL. Subsequently 100 µL of this suspension was seeded into 96-well plates and cells were allowed to adhere for 2 h at the standard conditions of 37 °C and 6% CO₂. Following the cell adhesion period, the buffer medium was aspirated and the SGM-buffered unfiltered PM extracts (mixed with a small volume of DCFH-DA solution (45 µM final concentration) were added to the cells. The macrophage exposure was carried out for 2.5 h under standard culturing conditions, after which the fluorescence intensity of each well was determined at 488 nm excitation and 530 nm emission using an M5e microplate reader (Molecular Devices, CA, USA). Raw fluorescence data were blank-corrected (cells without PM exposure) and normalized to the Zymosan (ZYM) positive controls (β-1,3 polysaccharide of D-glucose from Sigma Aldrich, MO, USA). Multiple dilutions (typically 4) of each sample were run, each in triplicate, to establish a linear portion of the dose response.

3. Results and discussion

3.1. Physical characteristics

As one facet of our investigation of the impacts of heating on concentrated ambient particles, their size distributions were measured before and after the thermodenuder, during both sampling periods. Fig. 2 illustrates the volume size distribution of the ambient and denuded particles, derived from the SMPS and OPS instruments merged at 0.3 μm , with the error bars corresponding to the variations in the ambient concentrations. As shown in the figure, heating the aerosol to 50 $^{\circ}\text{C}$ resulted in approximately 50% loss of the $\text{PM}_{2.5}$ vol (the total volume loss for particles with $d_p < 0.7 \mu\text{m}$ was 50.2% based on the SMPS data, while 48.5% loss was observed for particles in the range of 0.3–2.5 μm derived from OPS measurements). In addition, we measured around 50% losses in the volume concentrations of particles with $d_p < 0.1$, although this cannot be clearly observed in the figure due to the very low volume concentration of particles in this size range in comparison to the

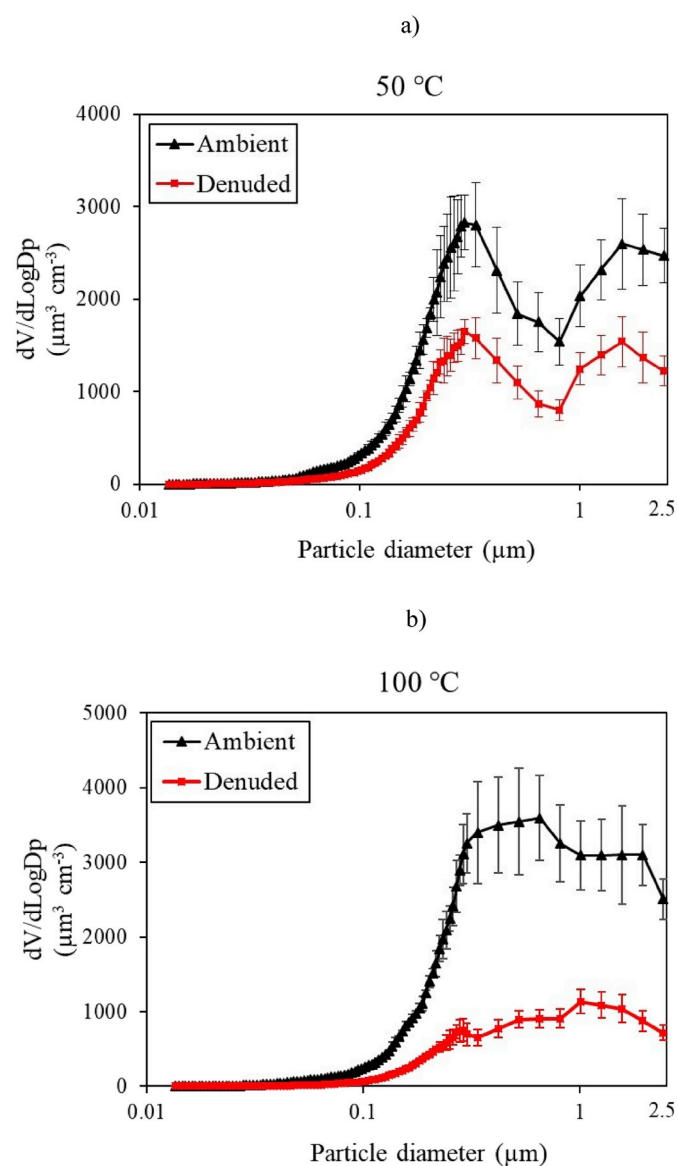


Fig. 2. Volume size distribution of the concentrated ambient and denuded $\text{PM}_{2.5}$ particles measured by SMPS and OPS at a) 50 $^{\circ}\text{C}$; and b) 100 $^{\circ}\text{C}$. The measured data from the two instruments is combined at 0.3 μm . The error bars correspond to one standard deviation.

larger particles. Moreover, heating the aerosol to 100 $^{\circ}\text{C}$ led to around 75% loss of the $\text{PM}_{2.5}$ vol (72.1% losses were observed in the total volume concentrations of particles with $d_p < 0.7 \mu\text{m}$ measured by the SMPS, whereas the corresponding value for particles in the range of 0.3–2.5 μm measured by the OPS was 77.2%). These results were further supported by the gravimetric data of the collected samples, with average mass concentration losses of 49.8% and 72.7% at temperature settings of 50 $^{\circ}\text{C}$ and 100 $^{\circ}\text{C}$, respectively. As noted earlier, heating the aerosol up to higher temperatures (i.e., 200 $^{\circ}\text{C}$) resulted in only small additional losses (up to 5–10% increase) in the total $\text{PM}_{2.5}$ concentrations, compared to the temperature configuration of 100 $^{\circ}\text{C}$. Thus, we selected 50 $^{\circ}\text{C}$ and 100 $^{\circ}\text{C}$ temperature settings for our detailed analysis on the volatility profile and toxicity of the semi-volatile components of $\text{PM}_{2.5}$.

3.2. Chemical components

3.2.1. EC, OC, and WSOC

Fig. 3(a–b) presents the measured concentrations of EC, OC, and WSOC in the ambient and denuded lines at different thermodenuder temperature settings for warm and cold periods, respectively. OC is comprised of a large number of organic components, most of which are known as semi-volatile compounds (SVOCs, referring to the compounds with vapor pressures at ambient temperatures in the range of 10^{-6} to 10^{-2} Pa (or, equivalently from 0.01 to 100 ppb), and can have significant concentrations in both the particulate and gas phases (Foreman and Bidleman, 1990). As shown in the figure, the $\text{PM}_{2.5}$ -bound OC concentrations were reduced by increasing the thermodenuder temperature to 50 $^{\circ}\text{C}$ and 100 $^{\circ}\text{C}$, documenting their semi-volatile nature. For instance, the warm phase OC concentration losses at 50 $^{\circ}\text{C}$ and 100 $^{\circ}\text{C}$ were 54% and 81%, respectively (Fig. 3(a)). The corresponding OC concentrations losses in the cold phase (55% and 80% losses at 50 $^{\circ}\text{C}$ and 100 $^{\circ}\text{C}$, respectively). Verma et al. (2011) reported losses of the OC in the quasi-ultrafine range due to heating of 35% and 40% at 50 $^{\circ}\text{C}$ and 100 $^{\circ}\text{C}$, respectively, in the warm phase - about 20–40% lower than the values derived in the current study. The organic species composition indicates an abundance of semi-volatile OC species such as, n-alkanes, PAHs, levoglucosan, and SOAs within the accumulation mode, consistent with earlier studies (Duan et al., 2012; Fine et al., 2004; Jimenez et al., 2009; Wang et al., 2009). For example, Fine et al. (2004) reported higher concentrations of levoglucosan (as a well-known tracer of biomass burning (Simoneit et al., 1999)) and 1,2-benzenedicarboxylic acid (as a tracer of photochemical SOA formation) in the accumulation mode as opposed to the UFP size range in an urban area located in Los Angeles.

Moreover, considerable losses were observed in the water extractable (WSOC) concentrations as a result of heating. In the warm phase, the concentration losses of WSOC were found to be 47% and 72% at the thermodenuder temperatures of 50 $^{\circ}\text{C}$ and 100 $^{\circ}\text{C}$, respectively. The corresponding WSOC losses in the cold phase were almost identical to those of the warm phase with 47% and 73% losses at 50 $^{\circ}\text{C}$ and 100 $^{\circ}\text{C}$, respectively. This finding is in agreement with the results of several studies in the literature (Hennigan et al., 2008; Matsunaga et al., 2005; Pun et al., 2002); for example, Hennigan et al. (2008) reported a mean value of 0.21 for the aerosol partition ratios (i.e., [particle]/[particle]+[gas]) of the measured WSOC concentrations in an urban region in Atlanta. Importantly, no significant loss was observed for EC concentrations upon heating of the aerosol, presumably due to the refractory nature of this component in the ambient air (Karanasiou et al., 2015; Schauer, 2003). Schauer (2003) reported that EC is a refractory component up to temperatures as high as 870 $^{\circ}\text{C}$, corroborating the non-volatility of this carbonaceous compound. It should be noted that the thermodenuder may have particle losses from temperature/size dependent processes such as diffusion and thermophoresis (Wehner et al., 2002). Using a thermodenuder with size dimensions and a flow rate comparable to that of our study, Wehner et al. (2002) reported

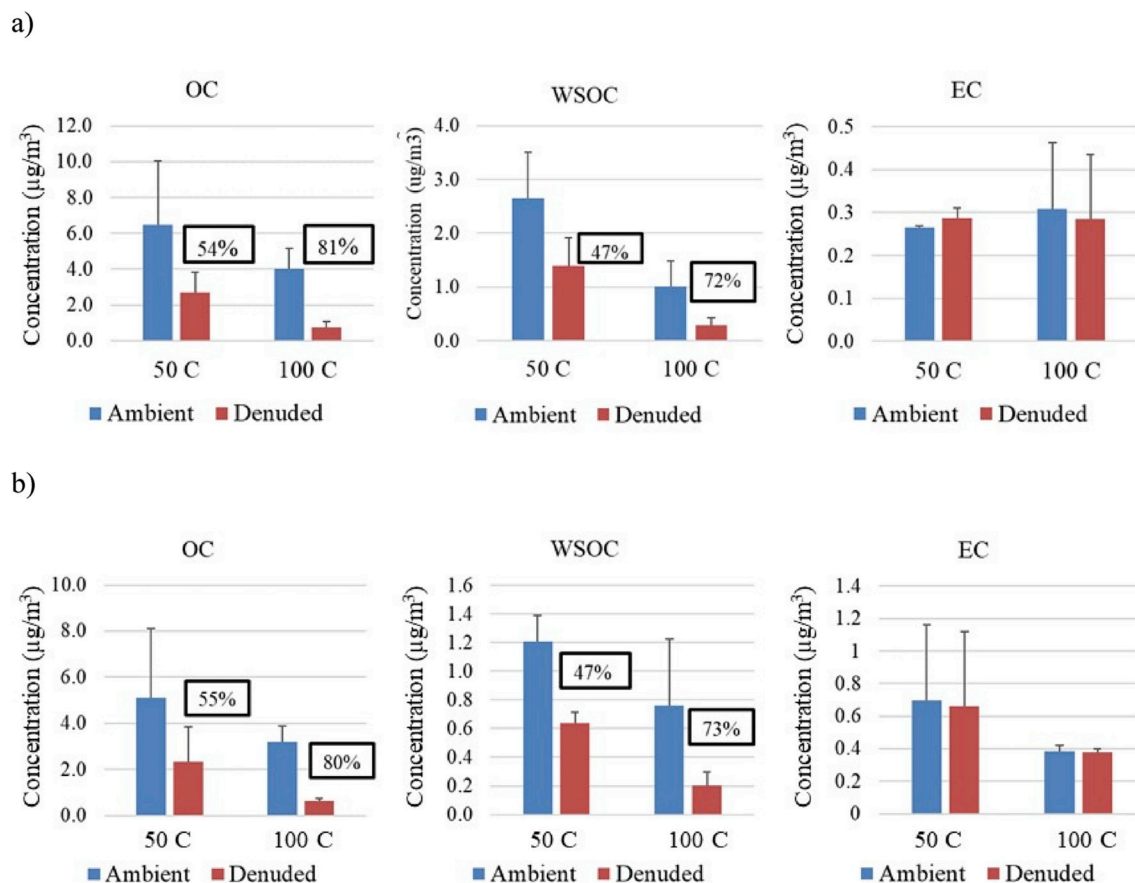


Fig. 3. Concentration of OC, WSOC, and EC in the ambient and denuded $PM_{2.5}$ at different temperatures: a) warm phase, b) cold phase. The percentages demonstrate the concentration loss as a result of heating. Error bars correspond to one standard deviation.

transmission efficiencies of around 80–100% for non-volatile Ag particles in the size range of <100 nm (i.e., the range that would be mostly affected by diffusional and thermophoretic losses) at temperature settings of 25 °C and 80 °C. Therefore, the losses at the temperature range adopted in this study (i.e., 50 °C and 100 °C) are expected to be negligible. This is further corroborated by the preservation of not only EC but of trace elements and metals at the various thermodenuder temperature settings (see Section 3.2.4).

3.2.2. Organic species

The concentration losses of certain organic species, including PAHs, organic acids, n-alkanes, and levoglucosan in the ambient and denuded lines are shown in Table 1. The average ambient concentrations of total PAHs, organic acids, n-alkanes, and levoglucosan were, respectively, 0.76, 291.55, 26.65, and 42.85 ng/m^3 in the winter phase; while their corresponding ambient concentrations in the summer phase were 0.03, 206.59, 13.47, and 9.23 ng/m^3 , respectively. The effect of thermodenuder heating on a given organic species was expected to be the same in warm and cold seasons, unless the matrix in which the species is bound

Table 1

Concentration losses for different categories of $PM_{2.5}$ organic compounds (and some of their individual species as example) as well as inorganic ions as a result of heating the aerosol to 50 °C and 100 °C. All values are reported as percentage (%).

Species	Warm phase		Cold phase			
	50 °C	100 °C	50 °C	100 °C		
Organic compounds	PAHs	Total range	56	80	55–64	72–91
		Pyrene	–	–	63	83
		Phenanthrene	56	80	60	79
		Fluoranthene	–	–	64	84
	Organic acids	Total range	43–61	69–94	40–66	67–88
		Decanoic Acid	54	69	56	68
		Dodecanoic Acid	55	77	53	81
		Hexadecanoic Acid	61	73	65	81
	n-alkanes	Total range	40–57	70–86	44–64	67–86
		n-Heneicosane	49	69	59	82
		n-Docosane	47	73	45	74
		n-Tricosane	55	76	52	71
Inorganic ions	Levoglucosan	51	71	60	92	
	Nitrate	66	89	64	88	
	Sulfate	49	71	54	71	
	Ammonium	53	84	59	92	

is quite different in the two seasons. To address this hypothesis, the results are presented for both warm and cold periods. Most of the investigated species showed comparable fractional losses in the warm and colder periods of our study, particularly at thermodenuder temperature of 50 °C. This lack of seasonal trend in PM fractional loss is consistent with the comparable OC volatility fractions (OCx) in warm and cold phases of our study (Fig. S1). OC1 to OC4 refer to the four temperature-resolved OC volatility fractions by the thermal/optical EC/OC analysis, with decreasing volatility from OC1 to OC4 (Chow et al., 2007). Results of a previous study at the same sampling site revealed that vehicular emissions are the dominant contributors to OC2 and OC3, while OC4 is dominated by secondary organic aerosol (SOA) formations (Soleimani et al., 2019). According to Fig. S1, the Chemical Speciation Network (CSN) data (Air Quality Data (PST) Query Tool, 2019) for different OC volatility fractions during our sampling periods (August 2018 as the warm period and late December 2018–early January 2019 as the colder period) showed only slight differences in the volatility profiles of ambient PM-bound organic matter in our sampling location across warm and colder phases of our study. The mass fractions of OC2, and OC3 (i.e., the more volatile fractions of OC) as well as OC4 (i.e., least volatile fraction of OC) were almost the same between the warm and colder phases. It should be noted that OC1 was not included in Fig. S1, since it has a much higher vapor pressure in comparison to the other OC fractions (Chow et al., 1993; Li et al., 2017), resulting in very low particle phase concentrations (in most cases below the detection limit) in the ambient conditions of Los Angeles.

Detailed explanations regarding concentration losses of each of the investigated groups (i.e., PAHs, organic acids, n-alkanes, and levoglucosan) in this study are presented in the following sections.

3.2.2.1. Polycyclic aromatic hydrocarbons (PAHs). PAHs are organic species with a wide range of volatility metrics, and mostly result from incomplete combustion in sources such as vehicular emissions and biomass burning (Shen et al., 2014). Regarding the specific study location, traffic emissions from the nearby freeway (i.e., I-110) have been shown to be the main source of these species in our sampling site (Ning et al., 2007; Saffari et al., 2016, 2015). In the warm phase, the concentration of most PAH compounds were below the limit of detection in the ambient and denuded lines, except for phenanthrene which is considered a tracer of vehicular emissions (Jang et al., 2013; Taghvaei et al., 2018). The phenanthrene concentration decreased upon heating in the thermodenuder, underscoring its semi-volatility origin. During the warm period, the concentration loss of phenanthrene at thermodenuder temperatures of 50 °C and 100 °C was 56% and 80%, respectively. During the cold period, a large suite of PAH were quantifiable, and, significant reductions were observed in the concentrations of all individual PAH species including phenanthrene (Phen), fluoranthene (Flt), pyrene (Pyr), chrysene (Chr), benzo(b)fluoranthene (BbF), benzo(k)fluoranthene (BkF), benzo(e)pyrene (BeP), indeno(1,2,3-cd) pyrene (Ind), and benzo(g,h,i)perylene (BghiP). The range of concentration losses for various PAHs in the cold phase were 55–64% and 72–91% at thermodenuder temperatures of 50 °C and 100 °C, respectively.

3.2.2.2. Organic acids. As shown in Table 1, we observed significant decreases in the concentrations of all organic acids due to the impact of heating in the thermodenuder. The percentage of mass loss for various organic acids were in the range of 43–61% and 69–94% at thermodenuder temperatures of 50 °C and 100 °C, respectively, in the warm phase. Similarly, the corresponding concentration losses for these species in the cold phase were 40–66% and 67–88%, respectively, at thermodenuder temperatures of 50 °C and 100 °C.

3.2.2.3. n-alkanes. The volatility characteristics and gas-particle partitioning of the straight-chain alkanes exhibit a broad range of values depending on carbon number (Yassaa et al., 2001). All of the n-alkanes

demonstrated concentration decreases upon heating in the thermodenuder setup (Table 1). The concentration losses for various n-alkanes in the warm phase were in the range of 40–57% and 70–86%, at thermodenuder temperatures of 50 °C and 100 °C, respectively. The corresponding range of concentration losses for these species were 44–64% and 67–86% at thermodenuder temperatures of 50 °C and 100 °C, respectively, in the cold phase.

3.2.2.4. Levoglucosan. Our results also revealed concentration reductions during both sampling periods for levoglucosan, a well-known tracer of biomass burning (Mochida et al., 2010; Simoneit et al., 1999; Zhang et al., 2008). In the warm period, the levoglucosan concentration losses at thermodenuder temperatures of 50 °C and 100 °C were 51% and 71%, respectively. The corresponding concentration losses in the cold phase were 60% and 92%, at thermodenuder temperatures of 50 °C and 100 °C, respectively.

3.2.3. Inorganic ions

Table 1 also presents the fractional concentration losses of the major inorganic ions, (nitrate, sulfate, and ammonium) upon heating for the warm and cold seasons. In the warm phase, at 50 °C, the concentration losses of nitrate, sulfate, and ammonium were 66%, 49%, and 53%, respectively, and even more pronounced at the higher thermodenuder temperature (i.e., 100 °C), 89%, 71% and 84% losses for nitrate, sulfate, and ammonium, respectively. The concentration losses in the cold phase for the above-mentioned inorganic ions, as shown in the Table 1, are quite comparable with those of the warm phase with only small differences of up to around 10%. Our results confirm the semi-volatile nature of these inorganic ions in an urban environment. This finding is consistent with the results of previous studies, investigating the formation of these species through gas/particle partitioning in various urban environments (Ansari and Pandis, 2000; Yao et al., 2003). Moreover, the reported losses of inorganic ions as well as OC in this study are comparable with the findings of a previous study conducted in the same sampling site (Verma et al., 2011) for the same temperature setting (i.e., 50 °C). The reported losses of quasi-UFP by Verma et al. (2011) were 35%, 49%, 44%, and 33% for OC, nitrate, ammonium, and sulfate, respectively. The small concentrations of these species remaining at higher temperatures (100 °C in the present study) might be due to the presence of more refractory forms of these components including Na₂SO₄ and NaNO₃ (Engler et al., 2007), which remain at particle phase even at higher temperatures. The observed losses for sulfate ions are higher than those of Huffman et al. (2008) study; thus, caution should be taken while reporting the sulfate losses. We cannot attribute these losses to temperature or size-dependent aerosol loss processes, such as thermophoresis and/or diffusion, based on the preservation of non-labile species, such as EC, trace elements and metals in PM_{2.5} at the different thermodenuder temperature settings. We also conducted controlled laboratory experiments with pure ammonium sulfate aerosols and observed similar losses at 50 °C (on average, 41.5%) (Fig. S2), which are in agreement with the reported sulfate losses in the field campaign. Verma et al. (2011) reported 33 ± 4% losses for sulfate at 50 °C in the same sampling location, which are lower, but not entirely out of range with the results of the current study, especially considering the much higher residence time of our denuder (i.e., 13 s) than that of Verma et al. (2011) (i.e., 0.7 s), the lower value of which might have resulted in incomplete evaporation. Lastly, the volatility of chloride was also investigated and minimal losses were observed at temperature settings of 50 °C and 100 °C (up to around 15%) during both seasons.

To further investigate the concentration losses of various semi-volatile species, a chemical mass balance analysis was conducted to compare the total PM_{2.5} mass loss to that of sum of the quantified species (i.e., EC, OC, organic species, inorganic ions, metals and trace elements). The average loss of the sum of quantified species was 39.4 ± 12.2% and 62.9 ± 7.1%, respectively, at temperature settings of 50 °C and 100 °C.

The losses are comparable to those of the total PM_{2.5} mass (P value of 0.3), corroborating our concentration loss results. The roughly 10% difference is most likely attributed to the unspiciated organics not included in our chemical analysis.

3.2.4. Metals and trace elements

The volatility profiles of a large number of inorganic elements (i.e., Na, Ca, Fe, K, Mg, Al, Ba, Ti, Cu, Zn, Mn, Cr, V, Ni, Co, and La) were also investigated in this study. The majority of these species had almost identical concentrations in the ambient and denuded lines at the different temperature settings. As an example, Fig. 4 illustrates the correlation analysis between the ambient and denuded concentrations for many of the different elements at the thermodenuder temperature of 100 °C in the warm phase. The slope and R² value of the regression line (Fig. 4) were 0.95 and 0.99, respectively, indicating the refractory nature of these elements at temperatures as high as 100 °C.

3.3. Oxidative potential

In Fig. 5, we present the oxidative potential (in units of $\mu\text{g Zymosan}/\text{m}^3$) of the collected PM samples in the ambient and denuded lines, during the warm and cold phases. The PM_{2.5} associated oxidative potential in the warm phase decreased by 44% upon thermodenuding at 50 °C. Therefore, almost half of the PM_{2.5} oxidative activity can be attributed to the semi-volatile species that are removed by heating the aerosol up to only 50 °C. However, it is conceivable that heating itself might result in some slight oxidative activity losses due to increased oxidation of reactive sites and redox changes, although earlier studies investigating oxidative potential of semi-volatile species have not taken into account this likely mechanism (Biswas et al., 2009; Miljevic et al., 2010; Verma et al., 2011). The oxidative potential of samples in the warm phase was further decreased by 29% (from 44% to 73%) upon increasing the temperature of the thermodenuder from 50 °C to 100 °C. Our findings also showed 56% and 85% reductions in the oxidative potential of cold period samples at temperatures of 50 °C and 100 °C, respectively. Although these (cold phase) reductions in oxidative

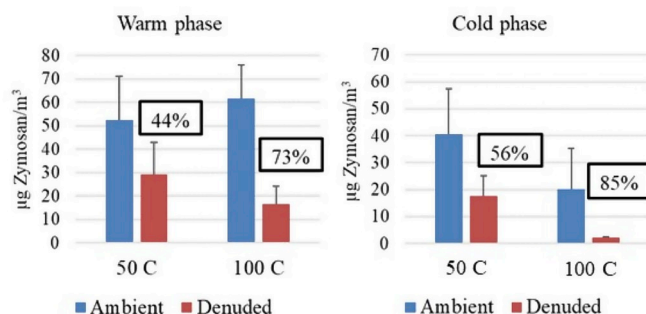


Fig. 5. Oxidative potential in the ambient and denuded PM_{2.5} at different temperature settings during the warm and cold seasons. The percentages demonstrate the oxidative potential reduction as a result of heating. Error bars correspond to one standard deviation.

potential for both temperature sets were around 12% higher than those of the warm phase samples, the seasonal difference was within variation of the data (P values ranging between 0.2 and 0.5). The comparable PM_{2.5} oxidative potential levels in the warm and colder phases of this study can be attributed to the seasonal variations in the concentrations of redox active organic compounds, some of which have higher concentrations in the winter (e.g., levoglucosan, and PAHs), and some in the summer (e.g., WSOC mostly due to the SOA formations).

3.4. Correlation analysis between PM_{2.5} oxidative potential and different PM chemical components

Bivariate correlation analyses were performed between the PM_{2.5} oxidative potential and different PM chemical components by calculating the Spearman non-parametric coefficients (summarized in Table 2). The PM_{2.5} oxidative potential showed a statistically significant correlation with OC for both the warm (R = 0.86, p = 0.003) and cold (R = 0.74, p = 0.018) phases of the study. This finding highlights the role of water soluble and insoluble PM_{2.5} organic compounds in inducing

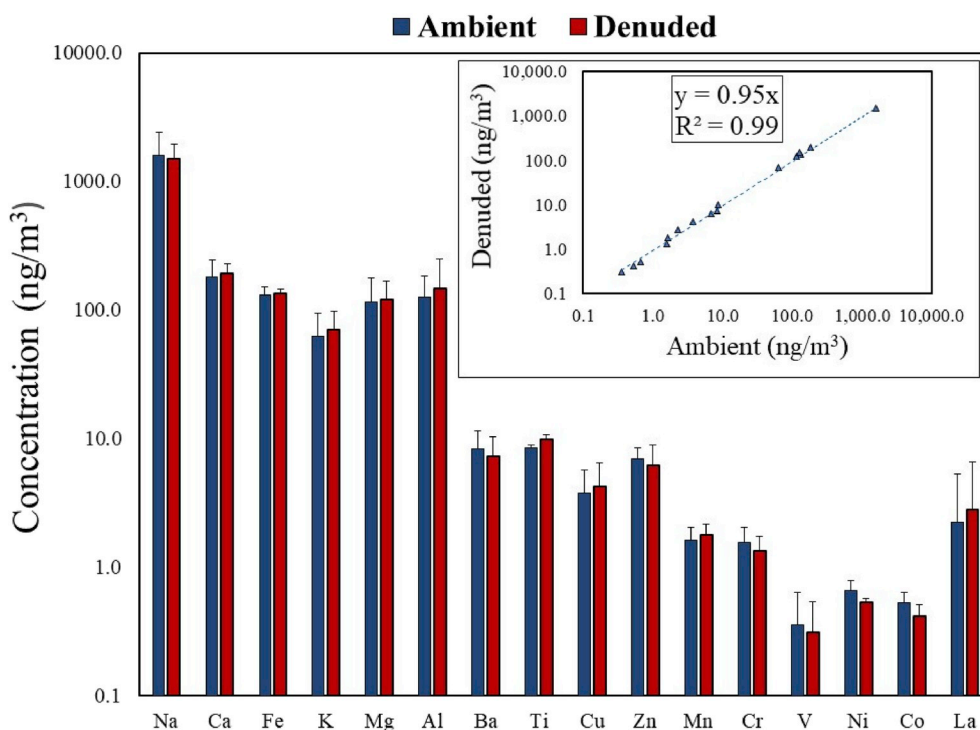


Fig. 4. Average concentrations of metals and trace elements in the ambient and denuded (at 100 °C) samples. Error bars correspond to one standard deviation. Linear regression of these components concentrations in the ambient vs. denuded line is also shown in the top corner of the figure.

Table 2

Spearman rank order correlation coefficients between the volumetric PM_{2.5} oxidative potential and major PM chemical components in the warm and cold seasons. R, n, and p values indicate the Spearman correlation coefficient, number of samples, and the associated level of significance, respectively.

Chemical components	Warm season (n = 8)		Cold season (n = 8)	
	R	p	R	p
OC	0.86	0.003	0.74	0.018
WSOC	0.60	0.060	0.98	0.001
Sum of the PAHs	0.88	0.002	0.76	0.014
Organic acids	0.76	0.014	0.88	0.002
n-alkanes	0.67	0.035	0.83	0.005
Levoglucosan	0.21	0.305	0.81	0.007
Nitrate	0.60	0.060	0.79	0.010
Sulfate	0.88	0.002	0.83	0.005
Ammonium	0.95	0.001	0.69	0.029

oxidative stress, as documented in several previous studies (Biswas et al., 2009; Cheung et al., 2009; Hu et al., 2009; Knecht et al., 2013; Ntziachristos et al., 2007; Samara, 2017; Styszko et al., 2017). WSOC was also highly correlated with the PM_{2.5} oxidative potential for both warm (R = 0.60, p = 0.06) and cold (R = 0.98, p = 0.001) periods mostly due to the active semi-volatile species of secondary origin formed during the photochemical oxidation of primary pollutants (Hennigan et al., 2008; Tuet et al., 2017). Also the strong correlation (R = 0.81) of levoglucosan (tracer of biomass burning activities (Argyropoulos et al., 2016; Hata et al., 2014) with the PM_{2.5} oxidative potential in the cold phase further corroborates the role of biomass burning during the colder phase of the study. The oxidative potential of PM_{2.5} was also highly correlated with insoluble organic species such as total PAH concentration, organic acids and n-alkane with R values ranging from 0.67 to 0.85.

Although inorganic ions showed strong correlations with PM oxidative potential, these are generally regarded as non-toxic species in the literature (Schlesinger and Cassee, 2003). By examining the correlation of the inorganic ions with other PM_{2.5} species, we found that these ions are strongly correlated with OC. The R values of correlation between nitrate, sulfate, ammonium and OC were in the range of 0.7–0.9 for both warm and cold phases. This finding suggests that the high correlation between inorganic ions and the PM oxidative potential might be due to their co-linearity with OC as a redox-active species. Similarly, Verma et al. (2011), have attributed the high correlation between inorganic ions and PM toxicity to the co-linearity of these components with ambient OC.

Finally, the remaining oxidative potential of the denuded samples at the thermodenuder temperature of 100 °C (around 15–25% on average) might be attributed to the presence of non-volatile compounds such as EC, transition elements and metals, which are not affected by heating and remained almost constant on all of the collected PM samples.

4. Summary and conclusions

In this study, we assessed the physicochemical characteristics and oxidative potential of PM_{2.5} semi-volatile species in a typical urban atmosphere impacted by a mixture of primary and secondary aerosols. Filter collection of concentrated ambient and thermodenuded fine particles was conducted using the VACES connected to a thermodenuder operated at 50 °C and 100 °C temperature settings. Corresponding PM_{2.5} mass losses through the denuder for the aforementioned temperature settings were around 50% and 75%, respectively. Our results show that PM components such as OC, WSOC, PAHs, organic acids, n-alkanes, levoglucosan, as well as inorganic ions (i.e., nitrate, sulfate, and ammonium) exhibit significant concentration losses (around 40%–90%) through the thermodenuder and this loss fraction was a function of temperature, whereas concentrations of the refractory species such as EC and most inorganic elements remained almost constant upon heating. A key finding of this study is the notable impact of semi-volatile

compounds on the ambient PM_{2.5} toxicity, as heating the aerosol to temperatures as low as 50 °C resulted in around a 50% reduction in the oxidative potential of PM_{2.5}. In conclusion, the reduction in the oxidative potential of PM_{2.5} due to thermodenuding was significantly correlated with the loss of semi-volatile organic compounds (i.e., WSOC, PAHs, organic acids, n-alkanes, and levoglucosan), which are marker species of aerosols of primary and secondary origins, further underscoring the need to implement stricter regulations to control the emissions and the subsequent health effects of the semi-volatile compounds.

Declaration of competing interest

The authors declare that they have no known competing financial interests or personal relationships that could have appeared to influence the work reported in this paper.

Acknowledgements

This study was supported by the National Institutes of Health (NIH) (grants number: 1RF1AG051521-01). The authors wish to thank the USC Viterbi School of Engineering's PhD fellowship award for their support.

Appendix A. Supplementary data

Supplementary data to this article can be found online at <https://doi.org/10.1016/j.atmosenv.2019.117197>.

References

- [WWW Document] Air Quality Data (PST) Query Tool, 2019, URL. <https://www.arb.ca.gov/aqmis2/aqselect.php?tab=specialrpt>.
- An, W.J., Pathak, R.K., Lee, B.-H., Pandis, S.N., 2007. Aerosol volatility measurement using an improved thermodenuder: application to secondary organic aerosol. *J. Aerosol Sci.* 38, 305–314.
- Ansari, A.S., Pandis, S.N., 2000. The effect of metastable equilibrium states on the partitioning of nitrate between the gas and aerosol phases. *Atmos. Environ.* 34, 157–168.
- Apte, J.S., Brauer, M., Cohen, A.J., Ezzati, M., Pope, C.A., 2018. Ambient PM_{2.5} reduces global and regional life expectancy. *Environ. Sci. Technol. Lett.* 5, 546–551. <https://doi.org/10.1021/acs.estlett.8b00360>.
- Argyropoulos, G., Besis, A., Voutsas, D., Samara, C., Sowlat, M.H., Hasheminassab, S., Sioutas, C., 2016. Source apportionment of the redox activity of urban quasi-ultrafine particles (PM_{0.49}) in Thessaloniki following the increased biomass burning due to the economic crisis in Greece. *Sci. Total Environ.* 568, 124–136.
- Bae, M.-S., Schauer, J.J., Lee, T., Jeong, J.-H., Kim, Y.-K., Ro, C.-U., Song, S.-K., Shon, Z.-H., 2017. Relationship between reactive oxygen species and water-soluble organic compounds: time-resolved benzene carboxylic acids measurement in the coastal area during the KORUS-AQ campaign. *Environ. Pollut.* 231, 1–12.
- Bates, J.T., Fang, T., Verma, V., Zeng, L., Weber, R.J., Tolbert, P.E., Abrams, J., Sarnat, S. E., Klein, M., Mulholland, J.A., 2019. Review of acellular assays of ambient particulate matter oxidative potential: methods and relationships with composition, sources, and health effects. *Environ. Sci. Technol.*
- Bi, X., Sheng, G., Peng, P., Chen, Y., Fu, J., 2005. Size distribution of n-alkanes and polycyclic aromatic hydrocarbons (PAHs) in urban and rural atmospheres of Guangzhou, China. *Atmos. Environ. Times* 39, 477–487.
- Birch, M.E., Cary, R.A., 1996. Elemental carbon-based method for monitoring occupational exposures to particulate diesel exhaust. *Aerosol Sci. Technol.* 25, 221–241.
- Biswas, S., Verma, V., Schauer, J.J., Cassee, F.R., Cho, A.K., Sioutas, C., 2009. Oxidative potential of semi-volatile and non-volatile particulate matter (PM) from heavy-duty vehicles retrofitted with emission control technologies. *Environ. Sci. Technol.* 43, 3905–3912.
- Brook, R.D., Rajagopalan, S., Pope III, C.A., Brook, J.R., Bhatnagar, A., Diez-Roux, A.V., Holguin, F., Hong, Y., Luepker, R.V., Mittleman, M.A., 2010. Particulate matter air pollution and cardiovascular disease: an update to the scientific statement from the American Heart Association. *Circulation* 121, 2331–2378.
- Cassee, F.R., Héroux, M.-E., Gerlofs-Nijland, M.E., Kelly, F.J., 2013. Particulate matter beyond mass: recent health evidence on the role of fractions, chemical constituents and sources of emission. *Inhal. Toxicol.* 25, 802–812.
- Chang, M.C., Sioutas, C., Kim, S., Gong Jr., H., Linn, W.S., 2000. Reduction of nitrate losses from filter and impactor samplers by means of concentration enrichment. *Atmos. Environ.* 34, 85–98.
- Charron, A., Harrison, R.M., 2003. Primary particle formation from vehicle emissions during exhaust dilution in the roadside atmosphere. *Atmos. Environ.* 37, 4109–4119.
- Cheng, H., Saffari, A., Sioutas, C., Forman, H.J., Morgan, T.E., Finch, C.E., 2016. Nanoscale particulate matter from urban traffic rapidly induces oxidative stress and

- inflammation in olfactory epithelium with concomitant effects on brain. *Environ. Health Perspect.* 124, 1537.
- Cheung, K.L., Polidori, A., Ntziachristos, L., Tzamkiozis, T., Samaras, Z., Cassee, F.R., Gerlofs, M., Sioutas, C., 2009. Chemical characteristics and oxidative potential of particulate matter emissions from gasoline, diesel, and biodiesel cars. *Environ. Sci. Technol.* 43, 6334–6340.
- Cho, A.K., Sioutas, C., Miguel, A.H., Kumagai, Y., Schmitz, D.A., Singh, M., Eiguren-Fernandez, A., Froines, J.R., 2005. Redox activity of airborne particulate matter at different sites in the Los Angeles Basin. *Environ. Res.* 99, 40–47.
- Chow, J.C., Watson, J.G., Chen, L.-W.A., Chang, M.C.O., Robinson, N.F., Trimble, D., Kohl, S., 2007. The IMPROVE_A temperature protocol for thermal/optical carbon analysis: maintaining consistency with a long-term database. *J. Air Waste Manag. Assoc.* 57, 1014–1023.
- Chow, J.C., Watson, J.G., Pritchett, L.C., Pierson, W.R., Frazier, C.A., Purcell, R.G., 1993. The DRI thermal/optical reflectance carbon analysis system: description, evaluation and applications in US air quality studies. *Atmos. Environ. Part A. Gen. Top.* 27, 1185–1201.
- Davidson, K., Hallberg, A., McCubbin, D., Hubbell, B., 2007. Analysis of PM_{2.5} using the environmental benefits mapping and analysis program (BenMAP). *J. Toxicol. Environ. Health Part A* 70, 332–346.
- Delfino, R.J., Staimer, N., Tjoa, T., Arhami, M., Polidori, A., Gillen, D.L., George, S.C., Shafer, M.M., Schauer, J.J., Sioutas, C., 2010. Associations of primary and secondary organic aerosols with airway and systemic inflammation in an elderly panel cohort. *Epidemiology* 21.
- Delfino, R.J., Staimer, N., Tjoa, T., Gillen, D.L., Schauer, J.J., Shafer, M.M., 2013. Airway inflammation and oxidative potential of air pollutant particles in a pediatric asthma panel. *J. Expo. Sci. Environ. Epidemiol.* 23, 466.
- Delgado-Saborit, J.M., Stark, C., Harrison, R.M., 2011. Carcinogenic potential, levels and sources of polycyclic aromatic hydrocarbon mixtures in indoor and outdoor environments and their implications for air quality standards. *Environ. Int.* 37, 383–392.
- Docherty, K.S., Stone, E.A., Ulbrich, I.M., DeCarlo, P.F., Snyder, D.C., Schauer, J.J., Peltier, R.E., Weber, R.J., Murphy, S.M., Seinfeld, J.H., 2008. Apportionment of primary and secondary organic aerosols in southern California during the 2005 study of organic aerosols in riverside (SOAR-1). *Environ. Sci. Technol.* 42, 7655–7662.
- Dockery, D.W., Stone, P.H., 2007. Cardiovascular risks from fine particulate air pollution. *N. Engl. J. Med.* 356, 511–513. <https://doi.org/10.1056/NEJMe068274>.
- Duan, J., Tan, J., Wang, S., Chai, F., He, K., Hao, J., 2012. Roadside, Urban, and Rural comparison of size distribution characteristics of PAHs and carbonaceous components of Beijing, China. *J. Atmos. Chem.* 69, 337–349.
- Engler, C., Rose, D., Wehner, B., Wiedensohler, A., Brüggemann, E., Gnauk, T., Spindler, G., Tuch, T., Birmili, W., 2007. Size distributions of non-volatile particle residuals (D_p < 800 nm) at a rural site in Germany and relation to air mass origin. *Atmos. Chem. Phys.* 7, 5785–5802.
- Ercal, N., Gurer-Orhan, H., Aykin-Burns, N., 2001. Toxic metals and oxidative stress part I: mechanisms involved in metal-induced oxidative damage. *Curr. Top. Med. Chem.* 1, 529–539.
- Fine, P.M., Chakrabarti, B., Krudysz, M., Schauer, J.J., Sioutas, C., 2004. Diurnal variations of individual organic compound constituents of ultrafine and accumulation mode particulate matter in the Los Angeles basin. *Environ. Sci. Technol.* 38, 1296–1304.
- Fine, P.M., Sioutas, C., Solomon, P.A., 2008. Secondary particulate matter in the United States: insights from the particulate matter supersites program and related studies. *J. Air Waste Manag. Assoc.* 58, 234–253. <https://doi.org/10.3155/1047-3289.58.2.234>.
- Foreman, W.T., Bidleman, T.F., 1990. Semivolatile organic compounds in the ambient air of Denver, Colorado. *Atmos. Environ. Part A. Gen. Top.* 24, 2405–2416.
- Gali, N.K., Yang, F., Cheung, C.S., Ning, Z., 2017. A comparative analysis of chemical components and cell toxicity properties of solid and semi-volatile PM from diesel and biodiesel blend. *J. Aerosol Sci.* 111, 51–64. <https://doi.org/10.1016/j.jaerosci.2017.06.005>.
- Gasser, M., Riediker, M., Mueller, L., Perrenoud, A., Blank, F., Gehr, P., Rothen-Rutishauser, B., 2009. Toxic effects of brake wear particles on epithelial lung cells in vitro. *Part. Fibre Toxicol.* 6, 30.
- Hasheminassab, S., Daher, N., Ostro, B.D., Sioutas, C., 2014a. Long-term source apportionment of ambient fine particulate matter (PM_{2.5}) in the Los Angeles Basin: a focus on emissions reduction from vehicular sources. *Environ. Pollut.* 193, 54–64. <https://doi.org/10.1016/j.envpol.2014.06.012>.
- Hasheminassab, S., Daher, N., Saffari, A., Wang, D., Ostro, B.D., Sioutas, C., 2014b. Spatial and temporal variability of sources of ambient fine particulate matter (PM_{2.5}) in California. *Atmos. Chem. Phys.* 14, 12085–12097.
- Hata, M., Chomanee, J., Thongyen, T., Bao, L., Tekasakul, S., Tekasakul, P., Otani, Y., Furuuchi, M., 2014. Characteristics of nanoparticles emitted from burning of biomass fuels. *J. Environ. Sci.* 26, 1913–1920.
- Hennigan, C.J., Bergin, M.H., Dibb, J.E., Weber, R.J., 2008. Enhanced secondary organic aerosol formation due to water uptake by fine particles. *Geophys. Res. Lett.* 35.
- Herner, J.D., Green, P.G., Kleeman, M.J., 2006. Measuring the trace elemental composition of size-resolved airborne particles. *Environ. Sci. Technol.* 40, 1925–1933.
- Hu, S., Fruin, S., Kozawa, K., Mara, S., Winer, A.M., Paulson, S.E., 2009. Aircraft emission impacts in a neighborhood adjacent to a general aviation airport in Southern California. *Environ. Sci. Technol.* 43, 8039–8045.
- Huffman, J.A., Ziemann, P.J., Jayne, J.T., Worsnop, D.R., Jimenez, J.L., 2008. Development and characterization of a fast-stepping/scanning thermodenuder for chemically-resolved aerosol volatility measurements. *Aerosol Sci. Technol.* 42, 395–407.
- Jang, E., Alam, M.S., Harrison, R.M., 2013. Source apportionment of polycyclic aromatic hydrocarbons in urban air using positive matrix factorization and spatial distribution analysis. *Atmos. Environ.* 79, 271–285.
- Jimenez, J.L., Canagaratna, M.R., Donahue, N.M., Prevot, A.S.H., Zhang, Q., Kroll, J.H., DeCarlo, P.F., Allan, J.D., Coe, H., Ng, N.L., Aiken, A.C., Docherty, K.S., Ulbrich, I.M., Grieshop, A.P., Robinson, A.L., Duplissy, J., Smith, J.D., Wilson, K.R., Lanz, V.A., Hueglin, C., Sun, Y.L., Tian, J., Laaksonen, A., Raatikainen, T., Rautiainen, J., Vaattovaara, P., Ehn, M., Kulmala, M., Tomlinson, J.M., Collins, D.R., Cubison, M.J., Dunlea, J., Huffman, J.A., Onasch, T.B., Alfarra, M.R., Williams, P.I., Bower, K., Kondo, Y., Schneider, J., Drewnick, F., Borrmann, S., Weimer, S., Demerjian, K., Salcedo, D., Cottrell, L., Griffin, R., Takami, A., Miyoshi, T., Hatakeyama, S., Shimo, A., Sun, J.Y., Zhang, Y.M., Dzepina, K., Kimmel, J.R., Sueper, D., Jayne, J.T., Herndon, S.C., Trimborn, A.M., Williams, L.R., Wood, E.C., Middlebrook, A.M., Kolb, C.E., Baltensperger, U., Worsnop, D.R., 2009. Evolution of organic aerosols in the atmosphere. *Science* 326, 1525–1529. <https://doi.org/10.1126/science.1180353>.
- Karanasiou, A., Mingüillón, M.C., Viana, M., Alastuey, A., Putaud, J.-P., Maenhaut, W., Panteliadis, P., Močnik, G., Favez, O., Kuhlbusch, T.A.J., 2015. Thermal-optical analysis for the measurement of elemental carbon (EC) and organic carbon (OC) in ambient air a literature review. *Atmos. Meas. Tech. Discuss.* 8.
- Kim, B.M., Cassmassi, J., Hogo, H., Zeldin, M.D., 2001. Positive organic carbon artifacts on filter medium during PM_{2.5} sampling in the South Coast Air Basin. *Aerosol Sci. Technol.* 34, 35–41.
- Kim, S., Jaques, P.A., Chang, M., Barone, T., Xiong, C., Friedlander, S.K., Sioutas, C., 2001a. Versatile aerosol concentration enrichment system (VACES) for simultaneous in vivo and in vitro evaluation of toxic effects of ultrafine, fine and coarse ambient particles Part II: field evaluation. *J. Aerosol Sci.* [https://doi.org/10.1016/S0021-8502\(01\)00058-1](https://doi.org/10.1016/S0021-8502(01)00058-1).
- Kim, S., Jaques, P.A., Chang, M., Froines, J.R., Sioutas, C., Barone, T., 2001b. Versatile aerosol concentration enrichment system (VACES) for simultaneous in vivo and in vitro evaluation of toxic effects of ultrafine, fine and coarse ambient particles Part I: development and laboratory characterization. *J. Aerosol Sci.* 32, 1299–1314. [https://doi.org/10.1016/S0021-8502\(01\)00057-X](https://doi.org/10.1016/S0021-8502(01)00057-X).
- Knecht, A.L., Goodale, B.C., Truong, L., Simonich, M.T., Swanson, A.J., Matzke, M.M., Anderson, K.A., Waters, K.M., Tanguay, R.L., 2013. Comparative developmental toxicity of environmentally relevant oxygenated PAHs. *Toxicol. Appl. Pharmacol.* 271, 266–275.
- Krasowsky, T.S., McMeeking, G.R., Wang, D., Sioutas, C., Ban-Weiss, G.A., 2016. Measurements of the impact of atmospheric aging on physical and optical properties of ambient black carbon particles in Los Angeles. *Atmos. Environ.* 142, 496–504.
- Landreman, A.P., Shafer, M.M., Hemming, J.C., Hannigan, M.P., Schauer, J.J., 2008. A macrophage-based method for the assessment of the reactive oxygen species (ROS) activity of atmospheric particulate matter (PM) and application to routine (daily-24 h) aerosol monitoring studies. *Aerosol Sci. Technol.* 42, 946–957.
- Li, H.Z., Dallmann, T.R., Li, X., Gu, P., Presto, A.A., 2017. Urban organic aerosol exposure: spatial variations in composition and source impacts. *Environ. Sci. Technol.* 52, 415–426.
- Li, N., Wang, M., Bramble, L.A., Schmitz, D.A., Schauer, J.J., Sioutas, C., Harkema, J.R., Nel, A.E., 2009. The adjuvant effect of ambient particulate matter is closely reflected by the particulate oxidant potential. *Environ. Health Perspect.* 117, 1116–1123.
- Lipsky, E.M., Robinson, A.L., 2006. Effects of dilution on fine particle mass and partitioning of semivolatile organics in diesel exhaust and wood smoke. *Environ. Sci. Technol.* 40, 155–162.
- Mader, B.T., Schauer, J.J., Seinfeld, J.H., Flagan, R.C., Yu, J.Z., Yang, H., Lim, H.-J., Turpin, B.J., Deminter, J.T., Heidemann, G., 2003. Sampling methods used for the collection of particle-phase organic and elemental carbon during ACE-Asia. *Atmos. Environ.* 37, 1435–1449.
- Matsunaga, S.N., Wiedinmyer, C., Guenther, A.B., Orlando, J.J., Karl, T., Toohey, D.W., Greenberg, J.P., Kajii, Y., 2005. Isoprene oxidation products are a significant atmospheric aerosol component. *Atmos. Chem. Phys. Discuss.* 5, 11143–11156.
- May, A.A., Presto, A.A., Hennigan, C.J., Nguyen, N.T., Gordon, T.D., Robinson, A.L., 2013a. Gas-particle partitioning of primary organic aerosol emissions: (1) Gasoline vehicle exhaust. *Atmos. Environ.* 77, 128–139.
- May, A.A., Presto, A.A., Hennigan, C.J., Nguyen, N.T., Gordon, T.D., Robinson, A.L., 2013b. Gas-particle partitioning of primary organic aerosol emissions: (2) Diesel vehicles. *Environ. Sci. Technol.* 47, 8288–8296.
- Miljevic, B., Heringa, M.F., Keller, A., Meyer, N.K., Good, J., Lauber, A., Decarlo, P.F., Fairfull-Smith, K.E., Nussbaumer, T., Burtcher, H., 2010. Oxidative potential of logwood and pellet burning particles assessed by a novel profluorescent nitroxide probe. *Environ. Sci. Technol.* 44, 6601–6607.
- Mochida, M., Kawamura, K., Fu, P., Takemura, T., 2010. Seasonal variation of levoglucosan in aerosols over the western North Pacific and its assessment as a biomass-burning tracer. *Atmos. Environ.* 44, 3511–3518.
- Mousavi, A., Sowlat, M.H., Hasheminassab, S., Polidori, A., Shafer, M.M., Schauer, J.J., Sioutas, C., 2019. Impact of emissions from the ports of Los Angeles and long beach on the oxidative potential of ambient PM_{0.25} measured across the Los Angeles county. *Sci. Total Environ.* 651, 638–647. <https://doi.org/10.1016/j.scitotenv.2018.09.155>.
- Mousavi, A., Sowlat, M.H., Sioutas, C., 2018. Diurnal and seasonal trends and source apportionment of redox-active metals in Los Angeles using a novel online metal monitor and Positive Matrix Factorization (PMF). *Atmos. Environ.* 174, 15–24.
- Ning, Z., Geller, M.D., Moore, K.F., Sheesley, R., Schauer, J.J., Sioutas, C., 2007. Daily variation in chemical characteristics of urban ultrafine aerosols and inference of their sources. *Environ. Sci. Technol.* 41, 6000–6006.

- Ning, Z., Moore, K.F., Polidori, A., Sioutas, C., 2006. Field validation of the new miniature versatile aerosol concentration enrichment system (mVACES). *Aerosol Sci. Technol.* **40**, 1098–1110. <https://doi.org/10.1080/02786820600996422>.
- Ntziachristos, L., Froines, J.R., Cho, A.K., Sioutas, C., 2007. Relationship between redox activity and chemical speciation of size-fractionated particulate matter. *Part. Fibre Toxicol.* **4**, 5.
- Ortega, A.M., Hayes, P.L., Peng, Z., Palm, B.B., Hu, W., Day, D.A., Li, R., Cubison, M.J., Brune, W.H., Graus, M., 2016. Real-time measurements of secondary organic aerosol formation and aging from ambient air in an oxidation flow reactor in the Los Angeles area. *Atmos. Chem. Phys.* **16**, 7411–7433.
- Pirhadi, M., Mousavi, A., Taghvaei, S., Sowlat, M.H., Sioutas, C., 2019. An aerosol concentrator/diffusion battery tandem to concentrate and separate ambient accumulation mode particles for evaluating their toxicological properties. *Atmos. Environ.* **213**, 81–89. <https://doi.org/10.1016/j.atmosenv.2019.05.058>.
- Pirhadi, M., Sajadi, B., Ahmadi, G., Malekian, D., 2018. Phase change and deposition of inhaled droplets in the human nasal cavity under cyclic inspiratory airflow. *J. Aerosol Sci.* **118**, 64–81. <https://doi.org/10.1016/j.jaerosci.2018.01.010>.
- Pope III, C.A., Muhlestein, J.B., Anderson, J.L., Cannon, J.B., Hales, N.M., Meredith, K.G., Le, V., Horne, B.D., 2015. Short-term exposure to fine particulate matter air pollution is preferentially associated with the risk of ST-segment elevation acute coronary events. *J. Am. Heart Assoc.* **4**, e002506.
- Pun, B.K., Griffin, R.J., Seigneur, C., Seinfeld, J.H., 2002. Secondary organic aerosol 2. Thermodynamic model for gas/particle partitioning of molecular constituents. *J. Geophys. Res. Atmos.* **107**, AAC-4.
- Riipinen, I., Pierce, J.R., Donahue, N.M., Pandis, S.N., 2010. Equilibration time scales of organic aerosol inside thermodenuders: evaporation kinetics versus thermodynamics. *Atmos. Environ.* **44**, 597–607.
- Robinson, A.L., Grieshop, A.P., Donahue, N.M., Hunt, S.W., 2010. Updating the conceptual model for fine particle mass emissions from combustion systems. *Allen L. Robinson. J. Air Waste Manage. Assoc.* **60**, 1204–1222.
- Saarikoski, S., Carbone, S., Cubison, M.J., Hillamo, R., Keronen, P., Sioutas, C., Worsnop, D.R., Jimenez, J.L., 2014. Evaluation of the performance of a particle concentrator for online instrumentation. *Atmos. Meas. Tech.* **7**, 2121–2135. <https://doi.org/10.5194/amt-7-2121-2014>.
- Saffari, A., Daher, N., Shafer, M.M., Schauer, J.J., Sioutas, C., 2014. Seasonal and spatial variation in dithiothreitol (DTT) activity of quasi-ultrafine particles in the Los Angeles Basin and its association with chemical species. *J. Environ. Sci. Heal. Part A* **49**, 441–451.
- Saffari, A., Hasheminassab, S., Shafer, M.M., Schauer, J.J., Chatila, T.A., Sioutas, C., 2016. Nighttime aqueous-phase secondary organic aerosols in Los Angeles and its implication for fine particulate matter composition and oxidative potential. *Atmos. Environ.* **133**, 112–122.
- Saffari, A., Hasheminassab, S., Wang, D., Shafer, M.M., Schauer, J.J., Sioutas, C., 2015. Impact of primary and secondary organic sources on the oxidative potential of quasi-ultrafine particles (PM_{0.25}) at three contrasting locations in the Los Angeles Basin. *Atmos. Environ.* **120**, 286–296.
- Saleh, R., Shihadeh, A., Khlystov, A., 2011. On transport phenomena and equilibration time scales in thermodenuders. *Atmos. Meas. Tech.* **4**, 571–581.
- Samara, C., 2017. On the redox activity of urban aerosol particles: implications for size distribution and relationships with organic aerosol components. *Atmosphere* **8**, 205.
- Sardar, S.B., Fine, P.M., Mayo, P.R., Sioutas, C., 2005. Size-fractionated measurements of ambient ultrafine particle chemical composition in Los Angeles using the NanoMOUDI. *Environ. Sci. Technol.* **39**, 932–944.
- Schauer, J.J., 2003. Evaluation of elemental carbon as a marker for diesel particulate matter. *J. Expo. Sci. Environ. Epidemiol.* **13**, 443.
- Schauer, J.J., Kleeman, M.J., Cass, G.R., Simoneit, B.R.T., 1999. Measurement of emissions from air pollution sources. 2. C1 through C30 organic compounds from medium duty diesel trucks. *Environ. Sci. Technol.* **33**, 1578–1587.
- Schlesinger, R.B., Cassee, F., 2003. Atmospheric secondary inorganic particulate matter: the toxicological perspective as a basis for health effects risk assessment. *Inhal. Toxicol.* **15**, 197–235.
- Senlin, L., Zhenkun, Y., Xiaohui, C., Minghong, W., Guoying, S., Jiamo, F., Paul, D., 2008. The relationship between physicochemical characterization and the potential toxicity of fine particulates (PM_{2.5}) in Shanghai atmosphere. *Atmos. Environ.* **42**, 7205–7214.
- Shafer, M.M., Hemming, J.D.C., Antkiewicz, D.S., Schauer, J.J., 2016. Oxidative potential of size-fractionated atmospheric aerosol in urban and rural sites across Europe. *Faraday Discuss* **189**, 381–405.
- Shen, H., Tao, S., Liu, J., Huang, Y., Chen, H., Li, W., Zhang, Y., Chen, Y., Su, S., Lin, N., 2014. Global lung cancer risk from PAH exposure highly depends on emission sources and individual susceptibility. *Sci. Rep.* **4**, 6561.
- Simoneit, B.R.T., Schauer, J.J., Nolte, C.G., Oros, D.R., Elias, V.O., Fraser, M.P., Rogge, W.F., Cass, G.R., 1999. Levoglucosan, a tracer for cellulose in biomass burning and atmospheric particles. *Atmos. Environ.* **33**, 173–182.
- Seimeanian, E., Mousavi, A., Taghvaei, S., Sowlat, M.H., Hasheminassab, S., Polidori, A., Sioutas, C., 2019. Spatial trends and sources of PM_{2.5} organic carbon volatility fractions (OC_x) across the Los Angeles Basin. *Atmos. Environ.* **209**, 201–211.
- Sowlat, M.H., Hasheminassab, S., Sioutas, C., 2016. Source apportionment of ambient particle number concentrations in central Los Angeles using positive matrix factorization (PMF). *Atmos. Chem. Phys.* **16**, 4849–4866. <https://doi.org/10.5194/acp-16-4849-2016>.
- Steenhof, M., Gosens, I., Strak, M., Godri, K.J., Hoek, G., Cassee, F.R., Mudway, I.S., Kelly, F.J., Harrison, R.M., Lebret, E., 2011. In vitro toxicity of particulate matter (PM) collected at different sites in The Netherlands is associated with PM composition, size fraction and oxidative potential—the RAPTES project. *Part. Fibre Toxicol.* **8**, 26.
- Steiner, S., Czerwinski, J., Comte, P., Popovicheva, O., Kireeva, E., Müller, L., Heeb, N., Mayer, A., Fink, A., Rothen-Rutishauser, B., 2013. Comparison of the toxicity of diesel exhaust produced by bio-and fossil diesel combustion in human lung cells in vitro. *Atmos. Environ.* **81**, 380–388.
- Stone, E.A., Snyder, D.C., Sheesley, R.J., Sullivan, A.P., Weber, R.J., Schauer, J.J., 2008. Source apportionment of fine organic aerosol in Mexico City during the MILAGRO experiment 2006. *Atmos. Chem. Phys.* **8**, 1249–1259.
- Styszko, K., Samek, L., Szramowiat, K., Korzeniewska, A., Kubisty, K., Rakoczy-Lelek, R., Kistler, M., Giebl, A.K., 2017. Oxidative potential of PM₁₀ and PM_{2.5} collected at high air pollution site related to chemical composition: krakow case study. *Air Qual. Atmos. Heal.* **10**, 1123–1137.
- Subramanian, R., Khlystov, A.Y., Cabada, J.C., Robinson, A.L., 2004. Positive and negative artifacts in particulate organic carbon measurements with denuded and undenuded sampler configurations special issue of aerosol science and technology on findings from the fine particulate matter supersites program. *Aerosol Sci. Technol.* **38**, 27–48.
- Taghvaei, S., Mousavi, A., Sowlat, M.H., Sioutas, C., 2019. Development of a novel aerosol generation system for conducting inhalation exposures to ambient particulate matter (PM). *Sci. Total Environ.* **665**, 1035–1045.
- Taghvaei, S., Sowlat, M.H., Hassanvand, M.S., Yunesian, M., Naddafi, K., Sioutas, C., 2018. Source-specific lung cancer risk assessment of ambient PM_{2.5}-bound polycyclic aromatic hydrocarbons (PAHs) in central Tehran. *Environ. Int.* **120**, 321–332.
- Tuet, W.Y., Chen, Y., Fok, S., Champion, J.A., Ng, N.L., 2017. Inflammatory responses to secondary organic aerosols (SOA) generated from biogenic and anthropogenic precursors. *Atmos. Chem. Phys.* **17**, 11423–11440.
- Verma, V., Ning, Z., Cho, A.K., Schauer, J.J., Shafer, M.M., Sioutas, C., 2009. Redox activity of urban quasi-ultrafine particles from primary and secondary sources. *Atmos. Environ.* **43**, 6360–6368.
- Verma, V., Pakbin, P., Cheung, K.L., Cho, A.K., Schauer, J.J., Shafer, M.M., Kleinman, M.T., Sioutas, C., 2011. Physicochemical and oxidative characteristics of semi-volatile components of quasi-ultrafine particles in an urban atmosphere. *Atmos. Environ.* **45**, 1025–1033. <https://doi.org/10.1016/j.atmosenv.2010.10.044>.
- Wang, D., Kam, W., Cheung, K., Pakbin, P., Sioutas, C., 2013a. Development of a two-stage virtual impactor system for high concentration enrichment of ultrafine, PM_{2.5} and coarse particulate matter. *Aerosol Sci. Technol.* **47**, 231–238.
- Wang, D., Pakbin, P., Shafer, M.M., Antkiewicz, D., Schauer, J.J., Sioutas, C., 2013b. Macrophage reactive oxygen species activity of water-soluble and water-insoluble fractions of ambient coarse, PM_{2.5} and ultrafine particulate matter (PM) in Los Angeles. *Atmos. Environ.* **77**, 301–310.
- Wang, G., Kawamura, K., Xie, M., Hu, S., Gao, S., Cao, J., An, Z., Wang, Z., 2009. Size-distributions of n-alkanes, PAHs and hopanes and their sources in the urban, mountain and marine atmospheres over East Asia. *Atmos. Chem. Phys.* **9**, 8869–8882.
- Wehner, B., Philippin, S., Wiedensohler, A., 2002. Design and calibration of a thermodenuder with an improved heating unit to measure the size-dependent volatile fraction of aerosol particles. *J. Aerosol Sci.* **33**, 1087–1093.
- Wittkopp, S., Staimer, N., Tjoa, T., Stinchcombe, T., Daher, N., Schauer, J.J., Shafer, M.M., Sioutas, C., Gillen, D.L., Delfino, R.J., 2016. Nrf2-related gene expression and exposure to traffic-related air pollution in elderly subjects with cardiovascular disease: an exploratory panel study. *J. Expo. Sci. Environ. Epidemiol.* **26**, 141.
- Yao, Y., Lau, A.P.S., Fang, M., Chan, C.K., Hu, M., 2003. Size distributions and formation of ionic species in atmospheric particulate pollutants in Beijing, China: 1—inorganic ions. *Atmos. Environ.* **37**, 2991–3000.
- Yassaa, N., Meklati, B.Y., Cecinato, A., Marino, F., 2001. Particulate n-alkanes, n-alkanoic acids and polycyclic aromatic hydrocarbons in the atmosphere of Algiers City Area. *Atmos. Environ.* **35**, 1843–1851.
- Zhang, R., Khalizov, A., Wang, L., Hu, M., Xu, W., 2011. Nucleation and growth of nanoparticles in the atmosphere. *Chem. Rev.* **112**, 1957–2011.
- Zhang, T., Claeys, M., Cachier, H., Dong, S., Wang, W., Maenhaut, W., Liu, X., 2008. Identification and estimation of the biomass burning contribution to Beijing aerosol using levoglucosan as a molecular marker. *Atmos. Environ.* **42**, 7013–7021.
- Zhang, X., McMurry, P.H., 1992. Evaporative losses of fine particulate nitrates during sampling. *Atmos. Environ. Part A. Gen. Top.* **26**, 3305–3312.
- Zhao, Y., Bein, K.J., Wexler, A.S., Misra, C., Fine, P.M., Sioutas, C., 2005. Field evaluation of the versatile aerosol concentration enrichment system (VACES) particle concentrator coupled to the rapid single-particle mass spectrometer (RSMS-3). *J. Geophys. Res. Atmos.* **110**.
- Žíková, N., Ondráček, J., Žďimal, V., 2015. Size-resolved penetration through high-efficiency filter Media typically used for aerosol sampling. *Aerosol Sci. Technol.* **49**, 239–249.